Mem. S.A.It. Vol. 75, 578

Memorie della

Heavy element abundances in AGB stars

The Hyades giants

E. C. Wylie, P. L. Cottrell and K. M. Taute

Department of Physics and Astronomy, University of Canterbury, Private Bag 4800, Christchurch, New Zealand
e-mail: e.wylie@phys.canterbury.ac.nz

Abstract. This research summarises our methodology for obtaining equivalent widths and abundances in giant stars. As an initial study, two of the four giants from the Hyades cluster have been analysed for heavy element abundances, specifically s-process elements. This paper displays the results obtained for HD28305 and HD27371, with most heavy element abundances proving to be the same in both stars and similar to those obtained in previous studies. The extension of these techniques to M, S and C stars is also discussed.

Key words. AGB stars – Hyades – s-process

1. Introduction: AGB stars

1.1. Thermal pulses

A star evolves onto the Asymptotic Giant Branch (AGB) after it has undergone He core burning and following H shell burning on the Red Giant Branch. The core of an AGB star consists of C and O surrounded by two He and H burning shells and a large convective envelope, as shown schematically in Figure 1. Periodically, the He shell undergoes a thermal runaway and produces vast amounts of energy, resulting in a thermal pulse, or shell flash (Lattanzio and Karakas 2001). This begins the 3rd dredge-up phase, during which the outer convective envelope penetrates the outer regions of the He shell and dredges the fresh carbon to the surface of the star. AGB stars experience several recurring thermal pulses during their lifetime. The main reason the AGB phase is so interesting to astrophysicists is the nucleosynthesis and element formation occurring throughout this phase.

Send offprint requests to: e.wylie@phys.canterbury.ac.nz

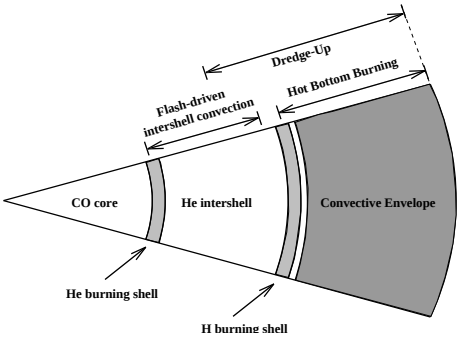

Fig. 1. Schematic of the internal structure of an AGB star (Lattanzio and Karakas 2001)

1.2. The formation of s-process elements

The s-process elements are formed by neutron capture which happens slowly relative to the corresponding beta decay. Observations have shown that most AGB stars are enriched in s-process elements. During the 3rd dredge-up phase, partial mixing occurs at the bottom of the shell and protons are deposited onto the convective envelope. These protons then combine with the ^{12}C present to form ^{13}C. If sufficient protons are present in this envelope the CN cycle proceeds and neutrons are produced when the ^{13}C reacts with helium. One of the consequences of this process is a layer of enhanced ^{13}C which forms in a region known as the ^{13}C pocket. This pocket is where the majority of the s-process element formation is thought to occur, with the addition of the excess neutrons onto seed nuclei (Lattanzio 2002), see Figure 2. During the next thermal pulse these s-process products are mixed into the convective envelope. It is this s-process overabundance, observed in the spectra of AGB stars, which provides direct evidence of the 3rd dredge-up phase.

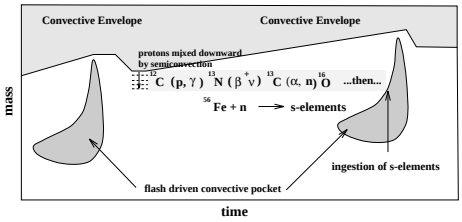

Fig. 2. Schematic showing the s-process in two consecutive thermal pulses (Lattanzio 2002).

2. Observations

All observations were taken with the 1m telescope at Mt John University Observatory in Tekapo, New Zealand, using the HERCULES high-resolution spectrograph (Hearnshaw et al 2002). A resolution of 35,000 was obtained for all exposures, with a S/N of at least 150.

2.1. Comparison test

In order to test the method chosen for equivalent width measurement and resulting abundance determinations, a comparison test was undertaken with a field supergiant, HD68752. For 57 spectral lines equivalent width measurements were obtained. These values were compared with those published by Gratton et al. (1989), see Figure 3. The equivalent width values obtained were then used as input for Kurucz's WIDTH9 program, which calculates abundances using a model atmosphere. The model atmosphere for HD68752 was found by interpolating between the cool star models of Bell et al. (1976). The resulting average abundances for each species were then compared to those published by Gratton et al. (1989), as shown in Figure 4. There was a high level of correlation between the two results, lending justification to the adopted techniques.

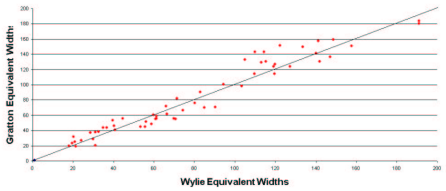

Fig. 3. Comparison test with results of equivalent widths published by Gratton et al. (1989) for the field giant HD68752.

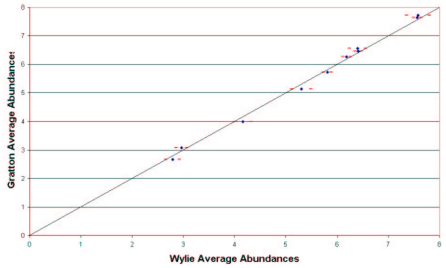

Fig. 4. Comparison test with results of average abundances published by Gratton et al. (1989) for the field giant HD68752.

3. Analysis and results: the Hyades giants

3.1. Results

Figures 5 and 6 show the preliminary results of this research, where the usual notation for [X] is adopted; [X]=log[X/H]$_*$-log[X/H]$_\odot$. These figures show previously published results (Boyarchuk et al. 2000) in smaller diamonds and the results from this research in larger, bold diamonds. Both stars show similar abundances for each element, which is expected given that they are from the same open cluster and are at the same evolutionary stage.

For iron, 60 lines were used to obtain the average abundance, which was found to be [Fe/H]=+0.18 and +0.19 for HD28305 and HD27371 respectively. The light s-process elements (Sr, Y, Zr) showed enhancements of ~0.1 dex with respect to the Sun, while the heavy s-process elements (Ba, La, Ce, Pr, Nd) showed abundances very close to that of the Sun. There are three likely sources of uncertainty in these average abundances, the largest being the spread in abundances obtained from various lines of the same species. For each line, synthetic spectra were calculated for abundances 0.1 dex either side of the final value. While this source of uncertainty is minimal for stronger lines, the uncertainty on weak lines is much greater as the difference between the synthetic spectra is often minimal. Uncertainty due to an inaccurate continuum is expected to be insignificant as the continuum was initially fitted by hand and then refined mathematically for each spectral order. The total uncertainty in the average abundances has been estimated at about ±0.07 dex at this stage but further analysis needs to be undertaken to refine this value.

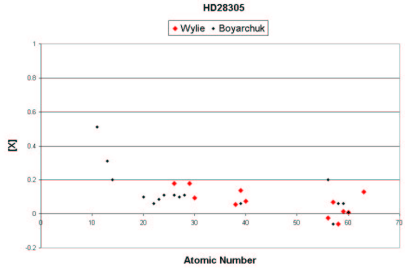

Fig. 5. Heavy element abundances for the Hyades giant HD28305.

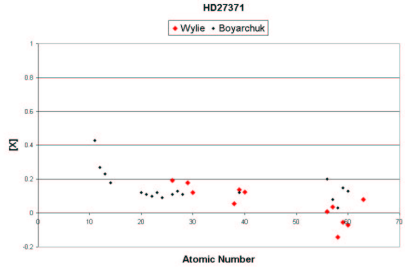

Fig. 6. Heavy element abundances for the Hyades giant HD27371.

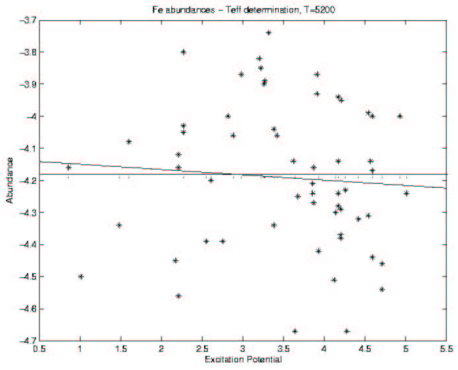

Fig. 7. Method used for determining effective temperature. If the temperature is chosen correctly the graph should show little or no trend.

3.2. Atmospheric modelling

In order to obtain abundances from the measured equivalent widths of spectral lines, it is necessary to define an accurate atmospheric model of the star in question. While the resulting abundances change only slightly with varying effective temperature, it is preferable to determine this parameter as accurately as possible. The plot of excitation potential and abundance for Fe lines aids in refining the effective temperature of the stellar atmospheric model chosen. If the chosen effective temperature is correct, the plot should display little or no trend, as is shown in Figure 7

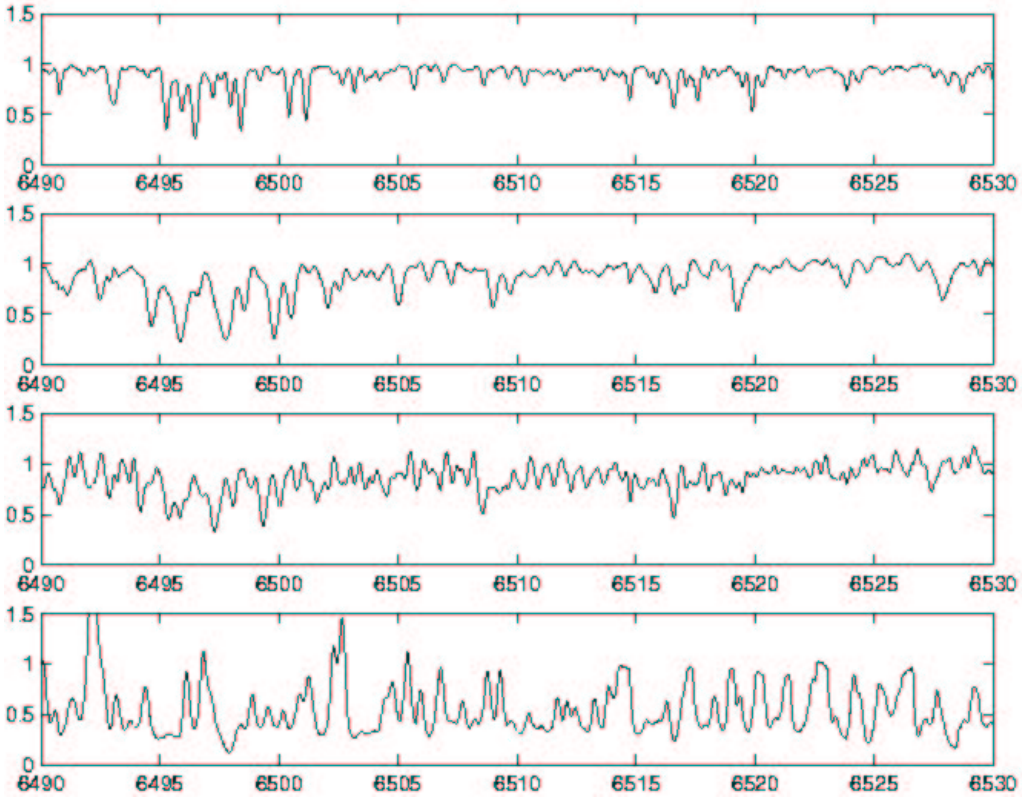

Fig. 8. Example of spectra from HD27371 (top) and M, S and C stars(top to bottom). The spectra becomes noticeably more crowded as the star moves up the AGB and increases its carbon content.

for HD27371 with an effective temperature of 5200 K. The effective temperatures decided on for this research were slightly different from those previously published (Boyarchuk et al. 2000) and were found to be 5100K and 5200K for HD28305 and HD27371 respectively.

3.3. Spectral line analysis

For both stars, fourteen heavy (A>26) element abundances were obtained, including the light and heavy s-process elements. Care was taken to select unblended lines. Where possible, unsaturated lines ($\log(W/\lambda) \leq -5$) were used to reduce the uncertainty due to incorrect microturbulence values. For unblended lines the equivalent width could be reliably measured using a gaussian approximation. These equivalent widths were then used as input for Kurucz's WIDTH9 atmospheric modelling program to give the corresponding abundance. The input atmospheric models required for this program were interpolated from the model grids provided by Bell et al. (1976).

While unblended lines were used where possible, most spectral lines of the heavier elements tended to be blended or very weak. In these cases spectrum synthesis was adopted to obtain accurate abundances. In order to ensure consistency and comparable abundances, a reverse solar analysis was undertaken using the UCLSYN synthesis program and the solar spectrum published in Beckers et al. (1976). For each line a fit was made to the solar spectrum using the accepted solar abundances adopted in Kurucz's ATLAS9 program (Kurucz 1970). For these accepted abundances

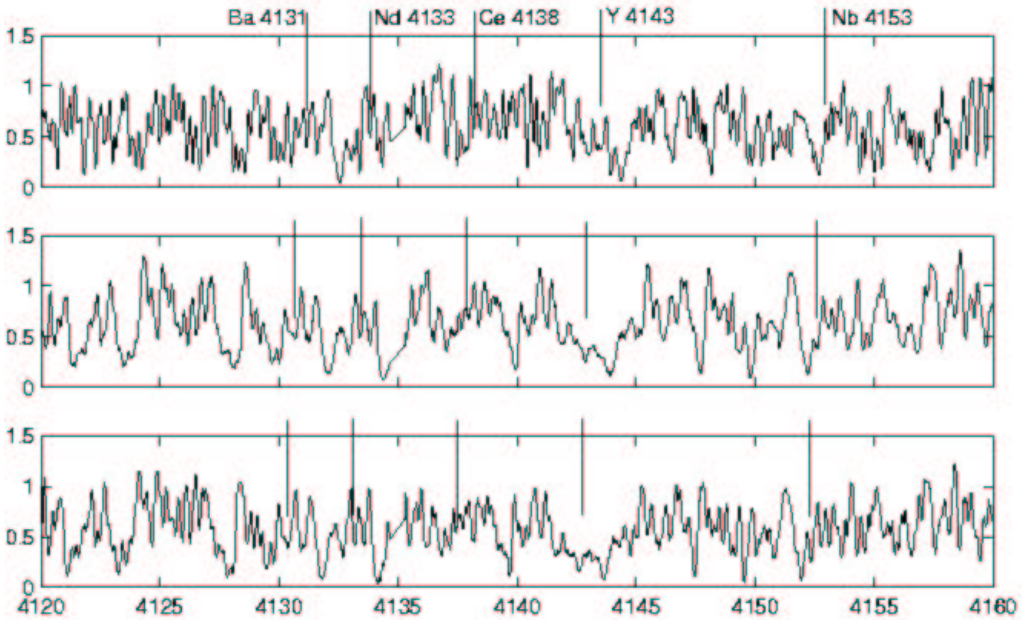

Fig. 9. Example of spectra from an M star (HD49331), an S star (HD30959) and a C star (HD 32736) showing the changes observed in specific s-process lines.

a corresponding log(gf) value was determined which provided the best fit to the observed solar spectrum. These adapted log(gf) values were then used in the synthesis of the lines for the two Hyades giants studied. This ensured consistency between the model grids used in the UCLSYN program and provided a way of obtaining reliable differential abundances.

4. The future: analysis of M, S, and C stars

Having explored the techniques of equivalent width measurement, atmospheric modelling and spectrum synthesis on the Hyades giants, we intend to use these same methods to determine s-process element abundances in AGB stars. As a star moves up the AGB it falls into one of five sub-groups - M, MS, S, SC, C - as its carbon content increases through dredge-up mixing. Several papers have investigated the enhancement of s-process elements along this branch (see Abia et al. 1998, 2001, 2002, 2003) and this research seeks to add to the existing observations.

4.1. Precautions and considerations

Due to their evolutionary phase, AGB stars present many difficulties when analysing the spectra and there are several precautions needed. The spectra of AGB stars quickly become crowded with molecular bands and metallic lines. This adds complications to spectrum synthesis of these stars as the modelling of molecular blanketing in these cool stars needs refining, despite improvements in model atmospheres for cool stars in general. Figure 8 shows a comparison between HD27371, a normal K giant, and the same region of an M, S and C star. The spectra quickly becomes noticeably more crowded.

While there is a marked increase in molecules and metallic lines present in the spectra of AGB stars, there is also a distinct change in the observable strength of s-process elements, which is what the research seeks to quantify.

Figure 9 shows the M, S and C sequence, with specific light (Y) and heavy (Ba, Nd, Ce) s-process element lines marked to show the observed change along the sequence.

The immediate research will concentrate on M, MS, S and SC stars and attempt to quantify the enhancements of s-process elements. While studies have been made of the separate subgroups, this research aims to provide a consistent study of the entire AGB phase. Analysis has already begun on field AGB stars and further observations are ongoing. An M star, HD 49331, and an S star, HD30959, are currently being analysed for s-process enhancements. Due to complications in the spectra of AGB stars, it is desirable to limit the amount of spectrum synthesis required to obtain s-process abundances. Investigations are underway to find a set of small (~10Å) regions which may provide us with relatively unblended s-process element lines needed to determine accurate abundances. Once these regions have been established, spectrum synthesis will be undertaken on numerous AGB stars of all sub-groups to obtain element abundances.

It is hoped that these observational results will then be compared directly to s-process yields predicted by the evolutionary modelling code, FRANEC (Chieffi and Straniero 1989). The comparison between observed and predicted s-process abundances will help to refine the parameters used in the modelling of the third dredge-up phase. It is the presentation of reliable observational evidence to assist in the modelling of the AGB phase which forms the ultimate goal of this research.

Acknowledgements. ECW is supported by a Department Ph.D. Scholarhsip, a University of Canterbury Research Award and the Dennis William Moore Scholarship.

References

Abia C., Wallerstein G., 1998, MNRAS, 293, 89

Abia C., Busso M., Gallino R., Domínguez I., Straniero O., Isern J., 2001, ApJ, 559, 1117

Abia C., Domínguez I., Gallino R., Busso M., Masera S., Straniero O., de Laverny P., Plez B., Isern J., 2002, ApJ, 579, 817

Abia C., Domínguez I., Gallino R., Busso M., Straniero O., de Laverny P., Wallerstein G., 2003, PASA, 20, 314

Beckers et al., 1976, A High-Resolution Spectral Atlas of the Solar Irradiance form 380 to 700 Nanometers, AFGT-TR-76-0126

Bell R.A., Eriksson K., Gustafsson B., Nordlund A, 1976, A&AS, 23, 37

Boyarchuk A.A., Antipova L.I., Boyarchuk M.E., Savanov I.S., 2000, Astro. Reports, 44, 76

Chieffi A., Straniero O., 1989, ApJS, 71, 49

Gratton R.G., Focardi P., Bandiera R., MNRAS, 1989, 214, 249

Hearnshaw, J.B., Barnes S.I., Kershaw G.M., Frost N., Graham G., Ritchie R., Nankivell G.R., Expt. Astr., 2002, 13, 59

Kurucz R.L., ATLAS: A computer program for calculating model stellar atmospheres, 1970, SAO Special Report 309

Lattanzio J.C., Karakas A.I., 2001, MmSAI, 72, 255

Lattanzio J.C., N.A. Reviews, 2002, 46, 469